

Resonant magnetotunneling through individual self-assembled InAs quantum dots

I. E. Itskevich,* T. Ihn, A. Thornton, M. Henini, T. J. Foster, P. Moriarty, A. Nogaret, P. H. Beton, L. Eaves, and P. C. Main

Department of Physics, University of Nottingham, Nottingham, NG7 2RD, United Kingdom

(Received 20 August 1996)

Resonant peaks are observed in the low-temperature current-voltage $I(V)$ characteristics of a single-barrier GaAs/AlAs/GaAs diode with InAs quantum dots incorporated in the AlAs tunnel barrier. We argue that each peak arises from single-electron tunneling through a *discrete zero-dimensional* state of an *individual* InAs dot in the barrier. Each peak splits into sharp components for magnetic field $B\parallel I$; the $I(V)$ curve probes the density of Landau-quantized states in the emitter-accumulation layer. A dot size of ≈ 10 nm was estimated from the diamagnetic peak shift for $B\perp I$. [S0163-1829(96)11848-8]

An array of quantum dots (QD's) produced by self-organized (Stranski-Krastanov) heteroepitaxial growth is formed when more than a critical layer thickness is grown on certain surfaces of different chemical composition and lattice constant. The system that has received the most attention to date consists of InAs dots grown on a GaAs or (AlGa)As surface.¹⁻¹² The electronic states of self-assembled dots capped by lattice matched layers have been investigated mainly by optical^{2,3,5,7,10-12} and capacitance^{5,6} spectroscopy. Due to variations in size, shape, and strain, a dot *ensemble* has a wide distribution of eigenenergies. Typically the optical spectra correspond to the dot *ensemble*;^{5,10-12} however, photoluminescence and cathodoluminescence spectra taken on submicron areas reveal emission lines corresponding to *individual* dots.^{2,3,7}

In this paper we report tunnel current investigations of the electron states in InAs quantum dots embedded in a thin AlAs layer of a single-barrier GaAs/AlAs/GaAs heterostructure. By tuning the applied voltage we can observe resonant tunneling through an *individual* dot. We use magnetotunneling spectroscopy to probe the initial and final states in the tunneling transition. We are also able to estimate the spatial extent of the confined electron wave function in the dot. In addition, the tunnel current through the localized state is also a sensitive probe of the properties of the electrons in the emitter contact.

Our device was prepared by first growing a 1- μm -thick GaAs buffer layer with graded Si doping on a (100) n^+ -GaAs substrate, followed by 100 nm of undoped GaAs and 5 nm of AlAs. The QD's were formed by growing 1.8 ML of InAs on the AlAs at a growth temperature of 520 °C. The dots were then nominally capped with a further 5 nm of AlAs, thus creating a 10-nm AlAs tunnel barrier. This was followed by an undoped 100-nm GaAs layer and capped by 1 μm of n^+ -GaAs of graded doping. Since we cannot exclude possible Al alloying, the dots should strictly be referred to as *In-based*, but for simplicity we henceforth refer to them as InAs QD's. A control sample, lacking the InAs layer but with other parameters identical, was also prepared. Circular mesas of various diameters, from 30 μm to 400 μm , were produced using optical lithography. AuGe was alloyed into the n^+ -GaAs layers to form Ohmic contacts.

To characterize the device, scanning electron and tunneling microscopy (SEM and STM) and photoluminescence (PL) spectroscopy were used. SEM and STM imaging was performed on samples of the same design but with the growth terminated after depositing the InAs layers. It allowed us to estimate the density of dots as $\approx 2 \times 10^{11}$ cm^{-2} , with a dot size $\approx (10 \times 10)$ nm^2 . A PL spectrum of our tunnel structure, recorded with a Ge detector using He-Ne laser excitation ($\lambda = 6328$ Å), is shown in the inset of Fig. 1. The spectrum exhibits a broad line with a maximum a few hundred meV below the GaAs band-gap energy. The line corresponds to the emission from the dot *ensemble* and is similar to that reported by other groups.^{2,11,12}

The expected conduction-band potential profile for our device is shown in Fig. 1. When a voltage V is applied between collector and emitter, a two-dimensional electron gas (2DEG), degenerate at low temperatures, accumulates in the undoped GaAs region adjacent to the tunnel barrier. Resonant tunnelling occurs if an electronic state of a QD in the barrier is resonant with a state in the 2DEG. Note that V is the external voltage applied to the device while the voltage drop V_1 between the 2DEG Fermi level and the states in the middle of the barrier is only a small fraction of V . As V_1 depends nonlinearly on V because of charge redistribution in the structure, we define the leverage factor f as $(dV_1/dV)^{-1}$.

The current-voltage characteristics $I(V)$, recorded for a

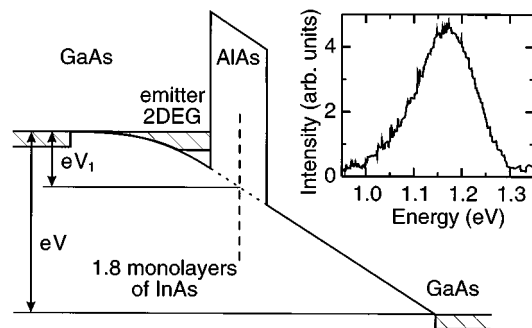


FIG. 1. A schematic energy band diagram of the sample under an applied voltage V . Inset: photoluminescence spectrum from the sample at 4.2 K.

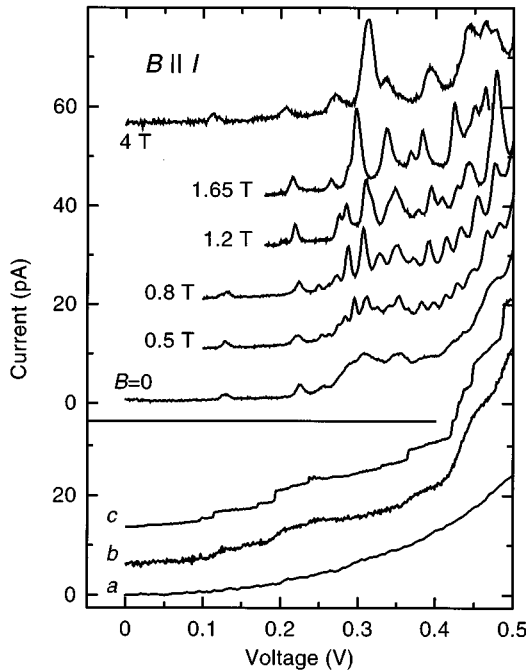


FIG. 2. The $I(V)$ characteristics of a $100\text{-}\mu\text{m}$ -diameter mesa. Lower: (a) control sample; (b) for $B=0$ in reverse bias at 4.2 K and (c) at 0.35 K . Upper: $I(V)$ in forward bias at 4.2 K at various $B\parallel I$. Curves are offset.

$100\text{-}\mu\text{m}$ -diameter mesa in the absence of magnetic field, are shown in Fig. 2. Forward and reverse bias correspond to electron flow from and to the substrate, respectively. An $I(V)$ curve for the control sample is also shown for comparison. Both devices have a very high impedance ($\sim 10^{12}\ \Omega$) around zero bias and exhibit a monotonically increasing background current. In addition, pronounced, low-current (a few pA) peaks, superimposed on the background current, are observed for the InAs quantum dot device for forward bias above 100 mV at 4.2 K . The peaks are absent in reverse bias at 4.2 K , where there is only indistinct structure. On lowering the temperature to 0.4 K , the structure in reverse bias evolves into a set of distinct steps. The $I(V)$ curve of the control sample has no structure in either bias direction but the background current is of similar magnitude.

The peaks in $I(V)$ arise from resonant tunneling through states in the barrier, and our observations indicate that these states are associated with the incorporation of InAs in the barrier. We argue that resonant tunneling occurs through discrete (zero-dimensional) electron states of individual InAs quantum dots in the barrier. To confirm this, we now examine the effect of magnetic field B on the tunneling current in forward bias. For B applied parallel to the current, the $I(V)$ curves change qualitatively as shown in Fig. 2. At fields as low as 0.4 T a series of narrow peaks arises in the curves. The peaks diverge in bias and their number falls with increasing B up to $3\text{--}4\text{ T}$. Increasing B from 4 to 12 T causes the peaks to shift to lower bias with little change in shape.

Figure 3(a) shows examples of $I(B)$ at constant bias V_0 . If V_0 is equal or close to the bias at which a peak occurs at 0 T , there are pronounced oscillations in $I(B)$. Their maxima and minima shift to smaller B with increasing V_0 . The $I(B)$ curves exhibit no structure at V_0 just below or above a peak in $I(V)$.

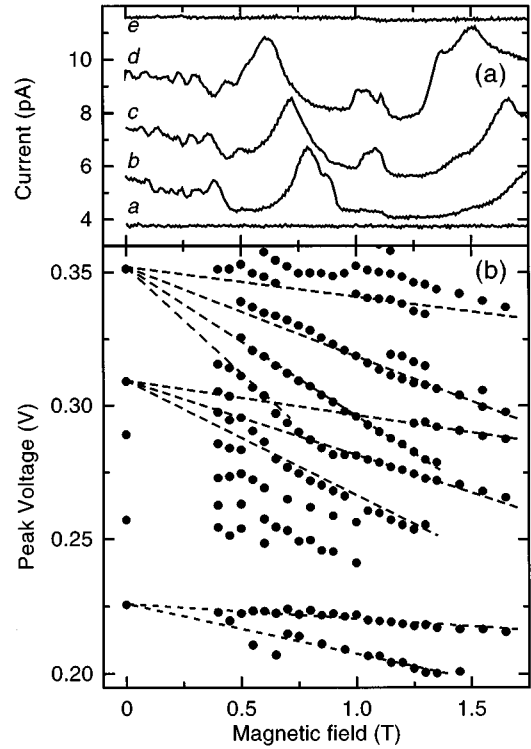


FIG. 3. (a) $I(B)$ characteristics at various V_0 : a, 105 mV ; b, 114 mV ; c, 115 mV ; d, 116 mV ; e, 130 mV . Curves are offset. (b) Fan chart of the peaks in $I(V)$ vs $B\parallel I$.

We attribute the sharp peaks in $I(V)$ to the Landau quantization of the 2DEG in the emitter which is consistent both with the peak divergence with increasing B and with their shift to lower V . As to the oscillations in $I(B)$, these behave quite differently from magneto-oscillations reported earlier in single-barrier tunneling devices,¹³ for which the maxima should shift to higher B with increasing V_0 . In our case a maximum in $I(B)$ occurs when the magnetic field brings an occupied Landau level in the 2DEG into resonance with an energy level in the barrier. In effect, both $I(V)$ and $I(B)$ probe the local density of states (DOS) of the 2DEG in the emitter accumulation layer.

This is illustrated in Fig. 3(b) by a fan chart of $I(V)$ -peak positions in the range of low B . Despite the complexity of the picture due to many overlapping lines, a distinct pattern emerges: the peaks shift to lower voltage, and there are a few sets of peaks diverging with B . The dashed lines are guides for the eye corresponding to possible Landau-level fans. The splitting (corresponding to the cyclotron energy) is different for each set due to the change in the electrostatic leverage with voltage (f varies from 7 to 12 in the voltage range shown; this is fully consistent with the sample electrostatic profile). Careful analysis of the peak positions and amplitudes provides no evidence for level repulsion effects. This indicates that each Landau-level fan originates from an independent dot. Occasionally, however, two peaks from different fans merge and it becomes difficult to trace the path of the peak with the smaller amplitude.

Note that the tunnel current can probe the DOS in the 2DEG at all energies; the technique is not confined to the Fermi energy. This has not been possible in previous experiments investigating resonant tunneling through quantum

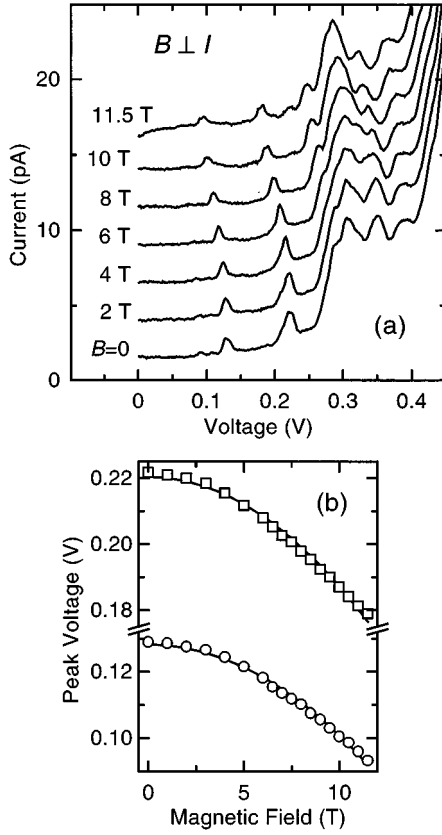


FIG. 4. (a) $I(V)$ characteristics at various $B \perp I$. Curves are offset. (b) Diamagnetic shift of lower-voltage peaks in $I(V)$. Solid lines are parabolic fits.

dots, due either to the larger size of the quantum dot¹⁴ or random disorder introduced by impurity states.¹⁵

Our $I(V)$ characteristics resolve the discrete DOS of 2D electrons where the cyclotron splitting is less than 1 meV. Such resolution is possible only if, for each Landau-level fan, the tunneling occurs through a *zero-dimensional* state in the barrier with a *discrete* energy level. Zero-dimensional states in the barrier might be due to donors, point defects or incorporated QD's. We reject the possibility of residual-donor-assisted tunneling, because there are no sharp features in $I(V)$ of the control sample. As to point defects that might arise in the barrier together with the dot formation, these would need to be very deep in energy relative to the AlAs conduction band and thus localized roughly on the scale of the lattice constant, which we show below is not the case.

To estimate the size of the resonant states in the barrier, we have used the diamagnetic shift of peaks in $I(V)$ in magnetic fields applied *normal* to the current. Applying B up to 11 T causes no qualitative change in the $I(V)$ characteristics at 4.2 K. Their evolution is shown in Fig. 4(a). The peak current values fall with increasing B for the lower-voltage peaks. The peak positions shift to lower voltage quadratically in B , as shown in Fig. 4(b).

The variation in peak voltage is determined by the relative diamagnetic shifts of the electron state in the 2DEG and the resonant state in the barrier, which provides information about its spatial extent. Hence

$$e\Delta V = -\frac{fe^2B^2}{2} \left(\frac{\langle z_e^2 \rangle}{m^*} - \gamma \frac{\langle z_d^2 \rangle}{m_d} \right).$$

Here $\sqrt{\langle z_e^2 \rangle} \approx 8$ nm is the spatial extent of the electron wave function in the emitter, estimated using self-consistent numerical calculations; $\sqrt{\langle z_d^2 \rangle}$ is the spatial extent of the barrier state; m^* and m_d are electron effective masses for the 2DEG and for the barrier state; γ is a geometrical factor arising from the zero-dimensional confinement ($\gamma=0.5$ for a spherically symmetric state), and f is the leverage factor. Using the GaAs Γ -valley effective mass, $0.067m_e$, both for m^* and m_d , $\gamma \approx 0.5$, and $f \approx 10$, consistent with the sample geometry, we estimate the size of the resonant barrier state $\Delta z_d \approx 2\sqrt{\langle z_d^2 \rangle} \approx (10 \pm 5)$ nm. The estimate is rather rough, because of uncertainty in the values of parameters used. Nevertheless, the estimate is *inconsistent* with strongly localized deep point defect states in the AlAs barrier. Conversely, it is fully consistent with the size of InAs QD's measured by SEM. Hence we conclude that each peak in $I(V)$ originates from tunneling through an electron state of a single self-assembled InAs dot incorporated in the barrier, analogous to tunneling through the impurity states.¹⁶

The observed decrease of peak amplitude with increasing $B \perp I$ in Fig. 4(a) is qualitatively similar to that reported recently for magnetotunneling into donor states.¹⁷ As will be discussed in another paper, this provides a separate estimate for the spatial extent of the dot wave function which is consistent with the above value.

The asymmetry of the $I(V)$ characteristics shown in Fig. 2 between *forward* and *reverse* bias results from the asymmetry of dot positions in the AlAs barrier. The dots are grown on the center plane of the barrier, but the covering AlAs layer is effectively thinner due to the size and shape of the dots. Thus for *reverse* bias the tunneling rate into a dot which may at high enough bias be dominated by inelastic processes is much greater than the rate of tunneling out. As each dot level moves below the emitter Fermi level, it gives rise to a distinct step in the $I(V)$ curve since it opens a new tunneling channel.¹⁸ Conversely, for *forward* bias the tunneling rate out of the dots is higher than the tunneling-in rate, and the current is a voltage-tunable probe of single-particle energy levels in the emitter.

The conclusion that each peak in $I(V)$ corresponds to tunneling through an *individual* dot is also supported by the peak current values. In this asymmetric geometry the tunnel current through a *single* dot can be written as $I = e\nu \exp(-2\kappa d)$, where ν is the attempt frequency, $d=5$ nm is the barrier half-thickness, $\hbar\kappa = \sqrt{2m^*\Delta E}$, and ΔE is the height of the barrier. Using the effective mass $m^* = 0.067m_e$ and $\Delta E \approx 0.8$ eV, expected for this heterostructure system, we obtain peak current values of a few pA, consistent with the experiment.

The question remains open as to why we observe tunneling through a single dot rather than the *ensemble* of about 10^7 dots in a typical mesa. The PL spectrum from the sample (Fig. 1) indicates that for the majority of dots the electron ground energy level is *below* the conduction-band edge E_c , in agreement with capacitance spectroscopy studies.⁶ These levels are unavailable for energy-conserving tunneling processes. Resonant tunneling processes probe only extremal dots with electron level energies *above* E_c . Such dots can arise due to fluctuations in size (30–40%), shape, strain, and AlAs coverage or possible Al alloying of dots. Our pic-

ture implies that a fraction of dots should be charged at zero bias, in order to align the chemical potentials of the dot *ensemble* and the collector and emitter *n*-doped contact layers. Under bias, the accumulation of the 2DEG is followed by the dot discharge, which contributes strongly to the leverage factor dependence on voltage.

In conclusion, we have observed resonant tunneling through single, independent electron states which are associated with self-assembled InAs quantum dots embedded in an AlAs matrix. The variation of the tunnel current with *B* pro-

vides information about the spatial extent of the dot wave function. In addition, the localized character of the electronic states means that the tunneling is also potentially a very sensitive way of probing the density of states in the emitter 2DEG, which has not been possible in previous experiments.

We are grateful to J. R. Middleton for processing the structures and to M. Steer and M. S. Skolnick for help with PL measurements and for useful discussions. This work is supported by EPSRC (U.K.). I.E.I. and L.E. acknowledge the Royal Society and EPSRC for financial support.

*On leave from the Institute of Solid State Physics, Russian Academy of Sciences, Chernogolovka, Moscow District, 142432, Russia.

¹J. M. Moison *et al.*, Appl. Phys. Lett. **64**, 196 (1994).

²J.-Y. Marzin *et al.*, Phys. Rev. Lett. **73**, 716 (1994).

³S. Fafard *et al.*, Phys. Rev. B **50**, 8086 (1994).

⁴D. Leonard, K. Pond, and P. M. Petroff, Phys. Rev. B **50**, 11 687 (1994).

⁵H. Drexler *et al.*, Phys. Rev. Lett. **73**, 2252 (1994).

⁶G. Medeiros-Ribeiro, D. Leonard, and P. M. Petroff, Appl. Phys. Lett. **66**, 1767 (1995).

⁷M. Grundmann *et al.*, Phys. Rev. Lett. **74**, 4043 (1995).

⁸S. Ruvimov *et al.*, Phys. Rev. B **51**, 14 766 (1995).

⁹M. Grundmann, O. Stier, and D. Bimberg, Phys. Rev. B **52**, 11 969 (1995).

¹⁰D. I. Lubyshv *et al.*, Appl. Phys. Lett. **68**, 205 (1996).

¹¹R. Heitz *et al.*, Appl. Phys. Lett. **68**, 361 (1996).

¹²M. Grundmann *et al.*, Appl. Phys. Lett. **68**, 979 (1996).

¹³F. W. Sheard, L. Eaves, and G. A. Toombs, Phys. Scr. **T19**, 179 (1987).

¹⁴B. Su, V.J. Goldman, and J.E. Cunningham, Phys. Rev. B **46**, 7644 (1992).

¹⁵P.J. McDonnell *et al.*, Physica B **211**, 433 (1995).

¹⁶A. Geim *et al.*, Phys. Rev. Lett. **72**, 2061 (1994).

¹⁷J.-W. Sakai *et al.*, Phys. Rev. B **48**, 5664 (1993).

¹⁸U. Meirav and E. B. Foxman, Semicond. Sci. Technol. **11**, 255 (1996).